Proceedings of the 35th Chinese Control Conference
July 27-29, 2016, Chengdu, China

Autonomous vehicle active safety system based on path planning and predictive control

Tianduo Xu, Hongliang Yuan

Abstract: Active safety systems have been identified as an effective technique for avoiding accidents. In this paper, in order to effectively avoid potential collisions, an active safety system consists of a motion planner and MPC-based active front steering and individual wheel force control is presented. The motion planner generates a polynomial parameterization trajectory for avoidance maneuver. Its analytical form render it being high computational efficiency. This feasible and smooth trajectory can be updated in real time once a potential collision in the environment is detected. Additionally, vehicle states at each time step can be derived from this trajectory analytically, hence the path planning algorithm can be well integrated into the following predictive control. To guarantee the reference trajectory can be well tracked, an MPC controller based on coupled longitudinal and lateral control is carried out to allocate the front steering angle and individual wheel forces. Finally, the simulations in Simulink environment confirm the effectiveness of the overall system.

Key Words: Collision avoidance, path planning, path tracking, model predictive control

1 Introduction

Recent trends in automotive industry point in the direction of increased content of electronics and computers, which strongly facilitates the development of Advanced Driver Assistance System(ADAS). ADAS are technologies that provide a driver with essential information, automate difficult or repetitive tasks, and lead to an overall increase in car safety for everyone. Active safety system, as an essential component of ADAS, can automatically detect potential collisions and offer drivers the option to let the vehicle take over the role as driver for collision avoidance. This technology has been acknowledged as an effective way particularly in emergency collision avoidance. For the sake of avoidance maneuver, a control strategy is proposed comprising three layers: environment sensing, path planning and path tracking. We assume the existence of a environment sensor and focus on path planning and tracking. Extensive researches have been done in these fields in the past.

Path Planning involves computing a continuous sequence of states/waypoints for a collision free path from start state to goal state while respecting the specified constraints[1]. There are various methodologies for path planning. Historically, the informed search algorithm A* and its various variants like D* Lite [2], Focussed D*[3] have been used for path planning. One advantage of the heuristic methods is that, if there is a path, it is guaranteed that it can be found. This can be proved theoretically. But the vehicle model is never a concern. The Genetic algorithm (GA)[4, 5] has been widely used due to its advantage of strong optimization ability and robustness. However, its main criticism lies in problems with respect to convergence. The RRT[6, 7] can provide a kinematically feasible path in continuous coordinate, whereas its efficiency largely depends on the choice of metric, which is equivalently difficult to optimization of the path. The problem with The artificial potential field method (APF)[8, 9] is that the vehicle can easily be trapped into local minima, which in general is inevitable, especially in a complex environment with multiple obstacles. The above mentioned algorithm are most employed in grid word. [10] proposes a method that analytically solve the problem of real time path planning, via generating a fifth-order polynomial to describe collision-free paths.

This paper develops a new polynomial parameterization method developed on the basis of a kinematic model of a car-like vehicle. The coefficients of the polynomials are determined by satisfying the boundary conditions and the vehicles kinematic model. Collision avoidance conditions are established and the algorithm can be updated in real time to obtain a collision-free path which is optimized by a minimum detour.

A complete active system involves a path tracking controller to assure the performance of the collision avoidance manoeuvre. Extensive research efforts have been focused on the path tracking problem[11, 12]. [13] adopts a fuzzy control approach to enhance the overall performance of automated steering. However, stability proof and performance analysis for this fuzzy control strategy are still difficult to establish. A neural network-based technique using genetic algorithm optimisation is proposed in [14]. The major drawback of this approach is the number of driving situations needed to build a representative training data set. [15] develops a Nonlinear Model-based Predictive Controller to handle lateral control. It offers satisfying performance for lateral guidance and preserves lateral stability during lateral maneuvers at high speed. However, the calculation time remains a strong burden for real-time applications. Moreover, MPC[16–19] is characterized with its ability of handling constraints in computation of the optimal solution, which makes MPC outperform other methods. However, most of the control strategies in them separate longitudinal and lateral control, wherein the MPC controller is primarily designed for lateral control.

The reference vehicle states at each time step could be accessed though the reference trajectory in this work, hence the longitudinal control could be integrated into the MPC controller design. With above ground truth, a coupled longitudinal and lateral controller based on MPC is proposed.

T. Xu is with the College of Electronics and Information Engineering, Tongji University, Shanghai 201804, China. email: 1433211@tongji.edu.cn

H. Yuan (corresponding author) is with the College of Electronics and Information Engineering, Tongji University, Shanghai 201804, China. e-mail: hyuan@tongji.edu.cn

The rest of the paper is organized as follows: the second section illustrates the research problem. The third section introduces the path-planning algorithm designed for generating a collision-free path. The fourth section presents the development of an MPC-based path tracking system. It actively controls the front steering and individual wheel forces to make the car track the generated trajectory. The effectiveness of the overall system is examined on Simulink platform in the fifth section.

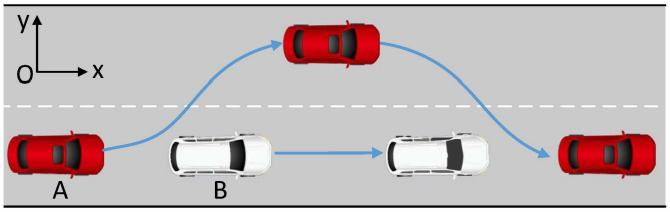

Fig. 1: A scenario of vehicle collision avoidance

2 Problem description

Fig. 1 shows a schematic example of a collision avoidance maneuver. Host vehicle A is moving at a higher speed v_0. It detects obstacle B ahead, which may be either moving slowly or stopped. To avoid a potential collision, the vehicle is going to perform a lateral maneuver, for which an evasive path must be planned and manipulated variables should be calculated for corresponding actuators.

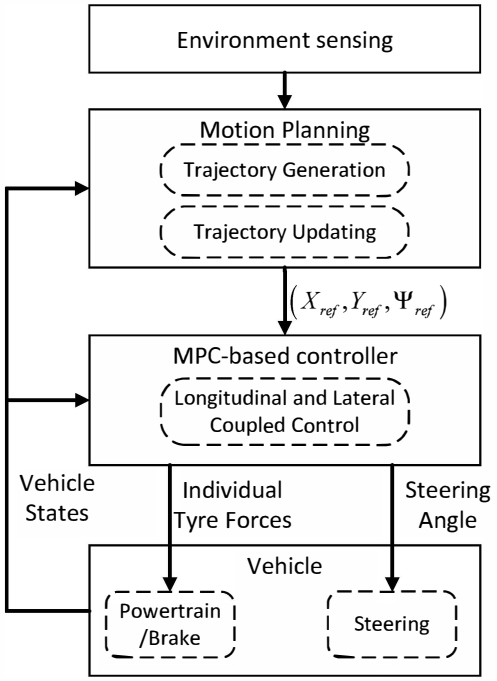

Fig. 2: Architecture of the active safety system

The architecture in Fig. 2 describes the main elements of the vehicle active safety system and it is composed of four modules: the environment sensor, the motion planner, the control system and the vehicle model. The trajectory generator plans and updates reference trajectories in real time based on current measurements. The control system commands the vehicle actuators involving steering angle, individual wheel forces based on reference states coming from the trajectory generators. Such reference states includes longitudinal and lateral positions, as well as yaw angle. The vehicle model is used to examine the performance of the active safety system.

3 Path planning

The design of trajectory generator and control system makes use of vehicle and environment models with different level of details, therefore a high-fidelity model is employed for designing the control system while the trajectory planner relies on a less detailed kinematic model, as show in Fig. 3.

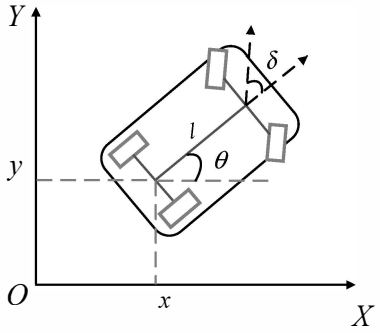

Fig. 3: Vehicle kinematic model

In Fig. 3, (x,y) are respectively the longitudinal and lateral position of the reference point P(at the midpoint of the rear axle) in the global coordinate system, θ is the yaw angle, δ is the front steering angle, v is the longitudinal vehicle speed, and l is the wheel base. The equations of motion are

$$\begin{aligned} \dot{x}(t) &= v\cos\theta(t) \\ \dot{y}(t) &= v\sin\theta(t) \\ \dot{\theta}(t) &= \frac{v\tan\delta(t)}{l} \end{aligned} \tag{1}$$

Let $q = (x, y, \theta, \delta, v, \dot{v})$ be the state vector of the vehicle, then the initial state is denoted as $q_0 = (x_0, y_0, \theta_0, \delta_0, v_0, \dot{v}_0)$, while the terminal state is $q_f = (x_f, y_f, \theta_f, \delta_f, v_f, \dot{v}_f)$. The initial and terminal time are denoted by t_0 and t_f respectively.

Assume (x_d(t), y_d(t)) defines the reference trajectory. Then the boundary conditions imposed on trajectory can be formed as

$$\begin{cases} x_d(t_0) = x_0 \\ \dot{x}_d(t_0) = v_0\cos\theta_0 \\ \ddot{x}_d(t_0) = \dot{v}_0\cos\theta_0 - \dfrac{v_0^2\tan\delta_0\sin\theta_0}{l} \end{cases}$$

$$\begin{cases} x_d(t_f) = x_f \\ \dot{x}_d(t_f) = v_f\cos\theta_f \\ \ddot{x}_d(t_f) = \dot{v}_f\cos\theta_f - \dfrac{v_f^2\tan\delta_f\sin\theta_f}{l} \end{cases}$$

$$\begin{cases} y_d(t_0) = y_0 \\ \dot{y}_d(t_0) = v_0\sin\theta_0 \\ \ddot{y}_d(t_0) = \dot{v}_0\sin\theta_0 + \dfrac{v_0^2\tan\delta_0\cos\theta_0}{l} \end{cases}$$

$$\begin{cases} y_d(t_f) = y_f \\ \dot{y}_d(t_f) = v_f\sin\theta_f \\ \ddot{y}_d(t_f) = \dot{v}_f\sin\theta_f + \dfrac{v_f^2\tan\delta_f\cos\theta_f}{l} \end{cases} \tag{2}$$

For the class of feasible trajectories $x_d(t)$, $y_d(t)$, boundary conditions in (2) represent six constraint equations for both x_d and y_d. Thus, function $x_d(t)$ and $y_d(t)$ are both chosen to be a polynomial of seventh order:

$$x_d(t) = \sum_{i=0}^{6} a_i t^i \qquad y_d(t) = \sum_{i=0}^{6} b_i t^i \tag{3}$$

Substituting equation (2) into equation (3) and solving the equations, the planned trajectory can be obtained as

$$\begin{aligned} x_d(t) &= f(t)L^{-1}(H_1 - Ma_6) + a_6 t_6 \\ y_d(t) &= f(t)L^{-1}(H_2 - Ma_6) + b_6 t_6 \end{aligned} \tag{4}$$

where

$$f(t) = [1 \quad t \quad t^2 \quad t^3 \quad t^4 \quad t^5]$$

$$H_1 = [x_d(t_0) \quad \dot{x}_d(t_0) \quad \ddot{x}_d(t_0) \quad x_d(t_f) \quad \dot{x}_d(t_f) \quad \ddot{x}_d(t_f)]^{\mathrm{T}}$$

$$H_2 = [y_d(t_0) \quad \dot{y}_d(t_0) \quad \ddot{y}_d(t_0) \quad y_d(t_f) \quad \dot{y}_d(t_f) \quad \ddot{y}_d(t_f)]^{\mathrm{T}}$$

$$M = [t_0^6 \quad 6t_0^5 \quad 30t_0^4 \quad t_f^6 \quad 6t_f^5 \quad 30t_4^f]^{\mathrm{T}}$$

$$L = \begin{pmatrix} 1 & t_0 & t_0^2 & t_0^3 & t_0^4 & t_0^5 \\ 0 & 1 & 2t_0 & 3t_0^2 & 4t_0^3 & 5t_0^4 \\ 0 & 0 & 2 & 6t_0 & 12t_0^3 & 20t_0^3 \\ 1 & t_f & t_f^2 & t_f^3 & t_f^4 & t_f^5 \\ 0 & 1 & 2t_f & 3t_f^5 & 4t_f^3 & 5t_f^4 \\ 0 & 0 & 2 & 6t_f & 12t_f^2 & 20t_f^4 \end{pmatrix}$$

In expression (4), a_6 and b_6 are left to be free variables. Thus the class of feasible trajectories have their polynomial parameterizations in terms of a_6 and b_6 to be determined. These two parameters could be determined by using collision-avoidance criterion, which is presented in forms of inequality as

$$(r_0 + r_1)^2 \leq [x_d(t) - x_0]^2 + [y_d(t) - y_0]^2 \tag{5}$$

where r_0 and r_1 are the vehicle radius and the obstacle radius respectively, x_0 and y_0 the obstacles position when detected.

Substituting the trajectory (4) into equation (5) and confining a_6 and b_6 on some straight lines such as $a_6 = 0$, $b_6 = 0, a_6 = b_6$ or $a_6 = -b_6$. For $b_6 = 0$, the solution for a_6 is:

$$\begin{aligned} a_6 \geq \max_{t\in[t_0,t_f]} \{ & \frac{\sqrt{(r_0 + r_1)^2 - [f_3 - y_0 - v_y(t - t_0)]^2}}{|f_1|} \\ & - \frac{f_2 - x_0 - v_x(t - t_0)}{f_1} \} = \bar{a}_6 \end{aligned} \tag{6}$$

or

$$\begin{aligned} a_6 \leq \max_{t\in[t_0,t_f]} \{ & -\frac{\sqrt{(r_0 + r_1)^2 - [f_3 - y_0 - v_y(t - t_0)]^2}}{|f_1|} \\ & - \frac{f_2 - x_0 - v_x(t - t_0)}{f_1} \} = \underline{a}_6 \end{aligned} \tag{7}$$

where v_x and v_y define the lead vehicle's velocity along the x and y directions. The last step is to propose a cost function to determine the value of a_6 and b_6, thereby an optimal trajectory is found out. By considering the difference between the planned trajectory and a straight line, such cost function is developed as

$$J(x_d, y_d) = \int_{t_0}^{t_f} [(x_d - x')^2 + (y_d - y')^2] dt \tag{8}$$

where

$$x' = k_x(t - t_0) \qquad y' = k_y(t - t_0)$$

$$k_x = \frac{x_f - x_0}{t_f - t_0} \qquad k_y = \frac{y_f - x_0}{t_f - t_0}$$

The cost function (8) integrates the difference between the planned trajectory and a straight-line trajectory and tries to minimize this difference. Thus, a optimal trajectory can be acquired by minimizing the cost function $J(x_d, y_d)$.

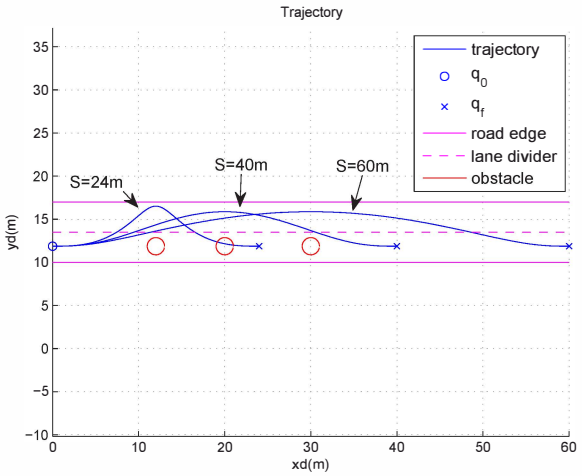

Fig. 4: Generated trajectories with set S={24m, 40m, 60m}, for: $\forall s \in S$, v=27km/h, t=6s

In real overtaking maneuver, the vehicle is supposed to have the terminal states, including velocity, acceleration, yaw angle, lateral position, equivalent to its initial state after a collision avoidance operation. With this consideration, we assume that $y_0 = y_f$, $v_0 = v_f$, $\theta_0 = \theta_f = 0$, $\dot{v}_0 = \dot{v}_f = 0$.

Fig. 4 presents a set of generated trajectories with different values of longitudinal distance S. The trajectory with $S = 24$m has a rapid variation in curvature that requires a large steering angle, while the one with $S = 60$m is smooth but has a long distance that commands a large acceleration. Both the two cases may violate vehicle physical limits. The middle one with $S = 40$m achieves the balance between the curvature and the distance of a path. On a basis of above analysis, the longitudinal distance S is a critical parameter related to the quality of planned trajectories.

With the definition that $y_0 = y_f$, $v_0 = v_f$, $\theta_0 = \theta_f = 0$, $\dot{v}_0 = \dot{v}_f = 0$, Table. 1 is made to serve as a reference for choosing an appropriate longitudinal distance S under different values of velocity and desired avoidance time. According to common vehicle models, physical limits are taken as $\dot{v}_{max} = 3.5m/s^2$ and $|\delta_{max}| = 30°$.

4 Vehicle control system design

In this section, we introduce the development of the MPC-based motion controller for the path tracking problem via active front steering and individual wheel force control. The tracking controller is based on two corner stones of vehicle modeling and control methodologies. Here, the motion of the vehicle is investigated in the yaw plane mainly describing the longitudinal and lateral motion. Therefore, a

Table 1: Initial parameters choosing

S(m) \ t(s) / v(km/h)	5	6	8	10
27	27∼51	31∼66	38∼98	45∼134
36	33∼64	38∼81	47∼119	56∼160
45	45∼77	52∼98	60∼138	68∼185
54	59∼89	67∼111	80∼158	89∼210
63	72∼102	83∼126	100∼178	114∼235
72	84∼114	98∼141	121∼198	139∼260

4WD vehicle model is developed for control design. This will be discussed in subsequent sections together with the design procedure of model predictive controller.

4.1 Vehicle modeling

This section is devoted to the description of the vehicle model(chassis and tyre) for the MPC regulator. The 4WD vehicle model employed here comprises three DoF for rigid body dynamics,that is, longitudinal, lateral and yaw degrees freedom. For the sake of compact notation, in the subsequent part, two subscript symbols are used to indicate variables related to the four wheels. Specifically, $* \in \{f, r\}$ denotes the front and rear axles, while $\diamond \in \{l, r\}$ denotes the left and right sides of the vehicle.

Let X and Y respectively be the longitudinal and lateral

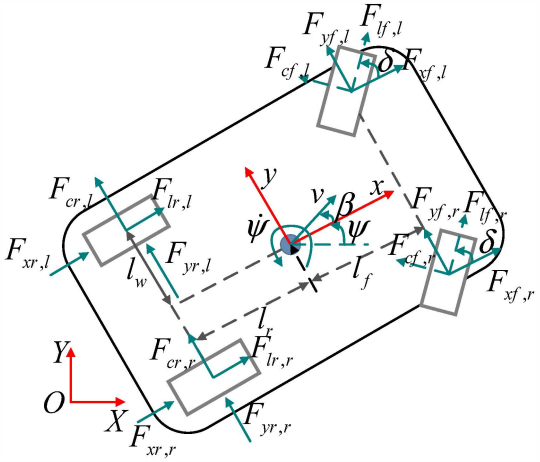

Fig. 5: The simplified vehicle model

directions in the global frame, x and y the longitudinal and lateral directions in the vehicle frame, ψ the yaw angle in the $\{x, y\}$ frame and Ψ the heading angle in the $\{X, Y\}$ frame, as illustrated by Fig. 5. By applying the Euler-Newton's formalism, the dynamic equations of the vehicle model are given by:

$$\begin{aligned} m\ddot{x} &= m\dot{y}\dot{\psi} + F_{x_{f,l}} + F_{x_{f,r}} + F_{x_{r,l}} + F_{x_{r,r}} \\ m\ddot{y} &= -m\dot{x}\dot{\psi} + F_{y_{f,l}} + F_{y_{f,r}} + F_{y_{r,l}} + F_{y_{f,r}} \\ I\ddot{\psi} &= l_f(F_{y_{f,l}} + F_{y_{f,r}}) - l_r(F_{y_{r,l}} + F_{y_{r,r}}) + \\ &\quad l_w(-F_{x_{f,l}} + F_{x_{f,r}} - F_{x_{r,l}} + F_{x_{r,r}}) \end{aligned} \tag{9}$$

where m and I are respectively the vehicle mass and the moment of inertia, l_f and l_r are the front and rear COG-distance, $F_{x_{*,\diamond}}$ and $F_{y_{*,\diamond}}$ are longitudinal and lateral tyre forces. The forces $F_{x_{*,\diamond}}$ and $F_{y_{*,\diamond}}$ depend on the longitudinal and lateral tire-road friction forces $F_{l_{*,\diamond}}$ and $F_{c_{*,\diamond}}$ as follows:

$$\begin{aligned} F_{x_{f,\diamond}} &= F_{l_{f,\diamond}} \cos\delta - F_{cf,\diamond} \sin\delta \\ F_{y_{f,\diamond}} &= F_{l_{f,\diamond}} \sin\delta + F_{c_{f,\diamond}} \cos\delta \\ F_{x_{r,\diamond}} &= F_{l_{r,\diamond}} \\ F_{y_{r,\diamond}} &= F_{c_{r,\diamond}} \end{aligned} \tag{10}$$

where δ the front steering angle. The chassis motion in the global frame is given by

$$\begin{aligned} \dot{X} &= \dot{x}\cos\Psi - \dot{y}\sin\Psi \\ \dot{Y} &= \dot{x}\sin\Psi + \dot{y}\cos\Psi \\ \dot{\Psi} &= \dot{\psi} \end{aligned} \tag{11}$$

The friction forces at the tire-road interface are the primal external forces acting on the vehicle dynamics. The longitudinal forces $F_{l_{*,\diamond}}$ mainly govern the longitudinal dynamics of the vehicle. For small value of slip ratio σ, $F_{l_{*,\diamond}}$ is a linear function in terms of $\sigma_{*,\diamond}$, which is given by

$$\begin{aligned} F_{l_{*,\diamond}} &= C_{\sigma_f}\sigma_{f,\diamond} \\ F_{l_{*,\diamond}} &= C_{\sigma_r}\sigma_{r,\diamond} \end{aligned} \tag{12}$$

where C_{σ_f} and C_{σ_r} are the front and rear longitudinal tyre stiffness respectively, and the slip ratio $\sigma_{*,\diamond}$ is defined as

$$\sigma_{*,\diamond} = \begin{cases} \dfrac{r_\omega\omega_{*,\diamond} - \dot{x}}{r_\omega\omega_{*,\diamond}} & \text{for acceleration} \\ \dfrac{r_\omega\omega_{*,\diamond} - \dot{x}}{\dot{x}} & \text{for braking} \end{cases} \tag{13}$$

where r_ω and $\omega_{*,\diamond}$ are the wheel radius and angular speed respectively. Similarly, for small values of slip angle, the relationship between slip angle and lateral force is linear. The slip angle indicates the angle between the wheel velocity and the direction of the wheel, which is defined as

$$\begin{aligned} \alpha_{f,l} &= \delta - \tan^{-1}\frac{\dot{y} + l_f\dot{\psi}}{\dot{x} - l_w\dot{\psi}} \quad \alpha_{r,l} = -\tan^{-1}\frac{\dot{y} - l_r\dot{\psi}}{\dot{x} - l_w\dot{\psi}} \\ \alpha_{f,r} &= \delta - \tan^{-1}\frac{\dot{y} + l_f\dot{\psi}}{\dot{x} + l_w\dot{\psi}} \quad \alpha_{r,r} = -\tan^{-1}\frac{\dot{y} - l_r\dot{\psi}}{\dot{x} + l_w\dot{\psi}} \end{aligned} \tag{14}$$

The lateral forces $F_{c_{*,\diamond}}$ are then obtained as

$$\begin{aligned} F_{c_{*,\diamond}} &= C_{\alpha_f}\sigma_{f,\diamond} \\ F_{c_{*,\diamond}} &= C_{\alpha_r}\sigma_{r,\diamond} \end{aligned} \tag{15}$$

where C_{α_f} and C_{α_r} are the front and rear tyre cornering stiffness respectively. Let $\xi = [\dot{x}\ \dot{y}\ \dot{\psi}\ \psi\ X\ Y]^{\mathrm{T}}$ defines the state, $u = [F_{l_{f,l}}\ F_{l_{f,r}}\ F_{l_{r,l}}\ F_{l_{r,r}}\ \delta]^{\mathrm{T}}$ represents the control input, and $o = [X\ Y\ \Psi]$ be the output. Combining the equations (9-15), the nonlinear vehicle model can be described by the following compact differential equation:

$$\begin{aligned} \dot{\xi} &= f(\xi(t), u(t)) \\ o &= h(\xi(t)) \end{aligned} \tag{16}$$

4.2 Longitudinal and lateral coupled control

Slip rate can be calculated based on tyre forces via making use of their linear proportional relationship. We assume the already existence of a low-level control that tracks slip rate and pay attention to the MPC controller. The basic idea of MPC is to use a prediction model to minimise the predicted difference between the future responses of a system and the desired responses, on a fixed finite time-horizon N_p named prediction horizon.

At time t_0, the system dynamics and initial conditions are known as:

$$\begin{aligned} \dot{\xi}_0 &= f(\xi_0, u_0) \\ \xi_0 &= \xi(t_0) \\ u_0 &= u(t_0) \end{aligned} \tag{17}$$

The linearised model can be approximated via applying Taylor series expansion on the nonlinear model near the initial point (ξ_0, u_0):

$$\Delta\dot{\xi}(t) = A(t)\Delta\xi(t) + B(t)\Delta u(t) \tag{18}$$

where, $\Delta\xi(t)$, $\Delta u(t)$, $A(t) \in R^{n\times n}$ and $B(t) \in R^{n\times m}$ are respectively defined as

$$\begin{aligned} \Delta\xi(t) = \xi(t) - \xi_0 \quad \Delta u(t) = u(t) - u_0 \\ A(t) = \frac{\partial f}{\partial \xi}|_{\xi_\bullet, u_\bullet} \quad B(t) = \frac{\partial f}{\partial u}|_{\xi_\bullet, u_\bullet} \end{aligned} \tag{19}$$

For simplicity, two new variables $\widetilde{\xi}$ and $\widetilde{u}$ are used to represent $\Delta\xi$ and Δu in the following part. The linearised model is rewritten as

$$\dot{\widetilde{\xi}} = A(t)\widetilde{\xi} + B(t)\widetilde{u} \tag{20}$$

where matrix A, B are coefficient matrixes. In standard MPC design, the prediction model is established based on a discrete system. Thus, we discretize the continuous model (20) and obtain

$$\widetilde{\xi}(k+1) = A_d\widetilde{\xi}(k) + B_d\widetilde{u}(k) \tag{21}$$

where $\widetilde{\xi} \in R^n$ is the state vector, $\widetilde{u} \in R^m$ is the control input.

The cost function is defined with two components: the predicted control inputs, the errors between desired outputs $\widetilde{o}_d(k)$ and predicted outputs $\widetilde{o}(k)$. Consider the following cost function

$$J = (R_s - \widetilde{O})^{\mathrm{T}} Q (R_s - \widetilde{O}) + \Delta\widetilde{U}^{\mathrm{T}} P \Delta\widetilde{U} \tag{22}$$

where $\widetilde{O} = [\widetilde{o}(k_i+1|k_i)^{\mathrm{T}}\ \widetilde{o}(k_i+2|k_i)^{\mathrm{T}}\ \widetilde{o}(k_i+3|k_i)^{\mathrm{T}} ... \widetilde{o}(k_i+N_p|k_i)^{\mathrm{T}}]^{\mathrm{T}}$ is the predicted outputs vector, $\Delta\widetilde{U} = [\Delta\widetilde{u}(k_i)^{\mathrm{T}}\ \Delta\widetilde{u}(k_i+1)^{\mathrm{T}}\ \Delta\widetilde{u}(k_i+2)^{\mathrm{T}} ... \Delta\widetilde{u}(k_i+N_c-1)^{\mathrm{T}}]^{\mathrm{T}}$ is optimization vector, $Q \in R^{N_\bullet \times N_\bullet}$ and $P \in R^{N_c \times N_c}\mathrm{T}$ are weighting matrices on the tracking errors and the control inputs, $R_s = [XY\Psi]$ is the reference vector, N_p and N_c are the prediction horizon and the control horizon respectively. The parameters N_p, N_c, Q and P are crucial for the stability of the MPC scheme. Additionally, in order to obtain a better performance, vehicle physical constraints involving limits of the tyre forces, the steering angle, the variation of steering angle, are supposed to be imposed on the model. With these considerations, the MPC problem is formulated as follows:

$$\begin{aligned} & \arg\min_{\Delta\widetilde{U}} J(\widetilde{\xi}(k), \Delta\widetilde{U}) \\ \text{s.t} \quad & \widetilde{\xi}(k+1) = A\widetilde{\xi}(k) + B\widetilde{u}(k) \\ & \widetilde{o}(k) = [\widetilde{X}(k)\widetilde{Y}(k)\widetilde{\Psi}(k)]^{\mathrm{T}} \\ & u_{min} \le u(k) \le u_{max} \\ & \Delta u_{min} \le \Delta u(k) \le \Delta u_{max} \end{aligned} \tag{23}$$

where u_{min} and u_{max} are the lower and upper bounds of the control input u, $\Delta 0 u_{min}$ and Δu_{max} are the lower and upper bounds of the control input variation.

5 Experiments

In this paper, the host vehicle checks to see whether the vehicle will collide with the obstacle at a constant frequency. The motion planner recomputes a new trajectory if a collision is detected, and in each computation, the terminal point is set in front of the obstacle with a fixed distance.

Two simulation scenarios: (A) Obstacle with constant velocity;(B) Obstacle with variable velocity, are carried out to evaluate the effectiveness of the overall system. In both scenarios, the initial velocity of the host vehicle(marked as triangles) is taken as 72km/h and that of the obstacle(marked as circles) is 18km/h. The control inputs are front tyre steering angles and longitudinal forces at four wheels.

5.1 Obstacle with constant velocity

To make the case more aggressive, the vehicle(triangles) is placed at (0, 2) as its initial position, while the desired trajectory for the vehicle at the beginning is a straight line starting from (0, 0), that is equivalent to imposing a disturbance on the controller. And obstacle is driving at (105, 0). The overall system tracking performance is captured in Fig. 6(a).

The MPC controller can quickly force the vehicle to steer back to the original lane, though with a large deviation. At 2s, the host vehicle is back to the original lane and detects the obstacle in advance at approximately 85m. Upon this, a trajectory is generated and the vehicle is controlled to follow it. The corresponding control commands for front tyre steering angle and individual wheel forces are show in Fig. (6(c)) respectively.

Dramatical changes of steering angle in early stage are observed in Fig. 6(c). This is believed to be caused by the large deviation from the reference trajectory. Since the MPC controller tries to minimize the difference quickly while constraints are imposed on the changing rate of steering angle, dramatical changes of commands to steering actuator is presented.

5.2 Obstacle with variable velocity

The vehicle is initially placed at (0, 0) and moves in a straight line. At 40m, a potential collision is detected, the path planning algorithm provides a reference trajectory and continuously check to see whether the vehicle will collide with the obstacle. At 6s, the obstacle speeds up. A collision will happen if the host vehicle continues to follow the initially planned trajectory. Upon detecting the impending collision,

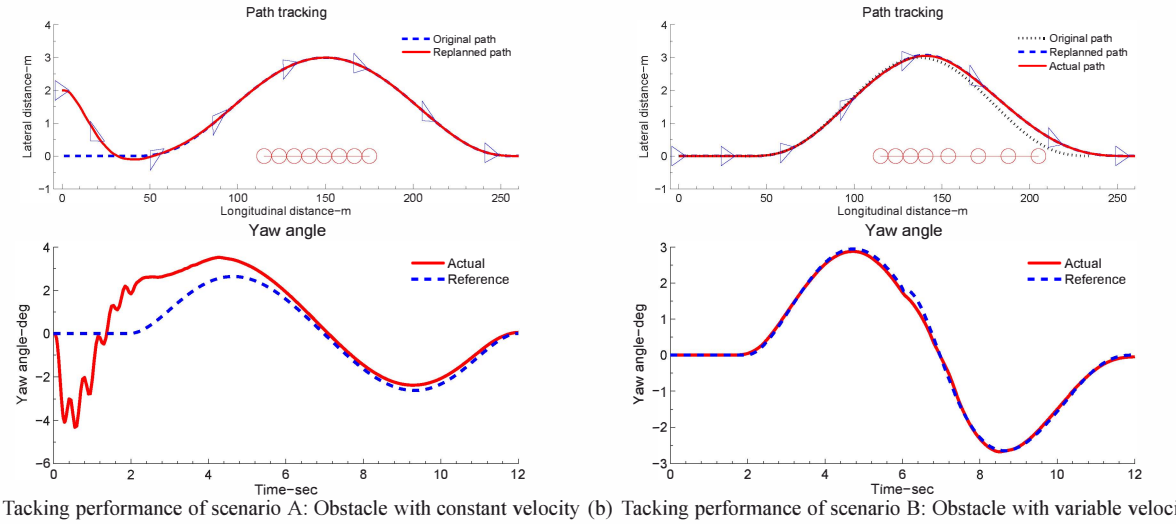

(a) Tacking performance of scenario A: Obstacle with constant velocity (b) Tacking performance of scenario B: Obstacle with variable velocity

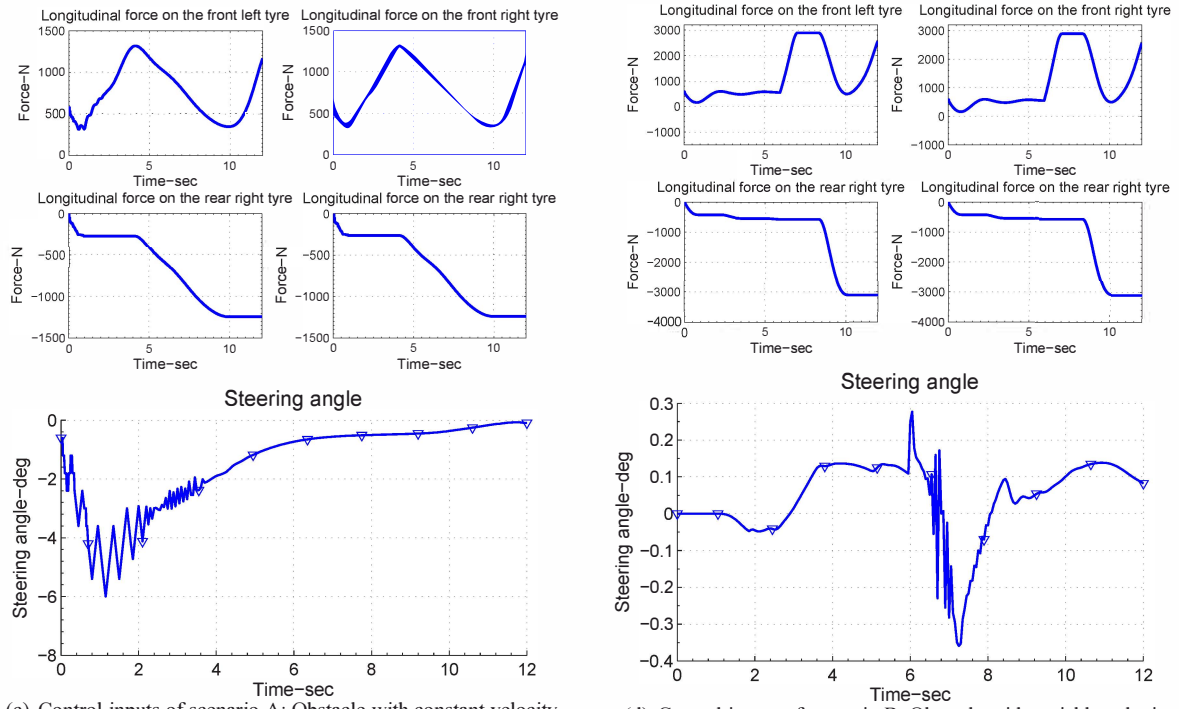

(c) Control inputs of scenario A: Obstacle with constant velocity (d) Control inputs of scenario B: Obstacle with variable velocity

Fig. 6: Simulation results

the motion planner recomputes a path and the vehicle takes up it. This is shown in Fig. 6(b).

It can be observed that the terminal way point of the replanned path is moved further ahead to avoid the obstacle which already accelerates from 18km/h to 36km/h. This process can be repeated until a collision-free trajectory is found. Fig. 6(d) shows the manipulated variables computed via MPC controller.

The recalculated trajectory guides the vehicle to move away from its original path at 6s, consequently a sudden higher command then followed by continuous fluctuations in steering angle appear at 6s. An increase in velocity is required to enable the host vehicle to overtake the accelerated obstacle. For that purpose, the controller demands a rise in front wheel forces to increase the velocity. Since we set the end velocity equivalent to initial velocity, the vehicle brakes when approaching final way point.

6 Conclusion

This paper proposes an active safety system for autonomous vehicle, using a two-level hierarchical architecture. The upper layer employs an analytical path planning algorithm to provide a collision-free path. Its most advantageous feature is in terms of extensibility. It can easily incorporate vehicle dynamics as well as stability criteria. The trajectory it computes contains vehicle states at each second. With this feature, it can well integrate with predictive control. The MPC layer makes use of a 4WD model to calculate control inputs for corresponding actuators. According to simulation results, the motion controller appears to be robust with respect to errors in reference variables. The path planner continuously checks impending collisions and provides reference trajectories for motion controller. The effectiveness of the overall control strategy is verified.

Lateral stability constraints are not yet incorporated in MPC controller design. A higher-fidelity predictive model is required to extend this controller to real vehicle control. For this purpose, the proposed scheme will be tested by Matlab-Carsim joint simulation platform in the future work. Meanwhile, a lower level for slip ratio control is still lacked. These issues are the subject of ongoing research.

7 Appendix

The parameters of the controller and the vehicle model used for simulations are given by the following tables:

Table 2: Vehicle model parameters

Parameter	Notation	Value
Vehicle mass	m	1542(kg)
Vehicle inertia moment	I	2786($kg \cdot m^2$)
Front-COG distance	l_f	1.77m
Rear-COG distance	l_r	0.92m
Vehicle wheelbase length	l_w	0.77m
Front tyre cornering stiffness	C_{α_f}	53000(N/rad)
Rear tyre cornering stiffness	C_{α_r}	44000(N/rad)

Table 3: MPC parameters

Parameter	Value
T	$50(ms)$
N_p	20
N_c	10
δ	$[-20°, 20°]$
$\Delta\delta$	$[-1°, 1°]$
$F_{l_{f/r,l/f}}$	$[-7422N, 7422N]$
$F_{c_{f/r,l/f}}$	$[-13867N, 0N]$
P_δ	10
$P_{F_{f,l/r}}$	5×10^{-6}
$P_{F_{r,l/r}}$	5×10^{-6}
P_X	1
Q_Y	1
Q_Ψ	10

References

[1] Dhiman N K, Deodhare D, Khemani D. A review of path planning and mapping technologies for autonomous mobile robot systems[C]// Proceedings of the 5th ACM COMPUTE Conference: Intelligent & scalable system technologies. ACM, 2012.

[2] Koenig S, Likhachev M. Fast replanning for navigation in unknown terrain[J]. IEEE Transactions on Robotics, 2005, 21(3):354-363.

[3] Stentz A. The Focussed D* Algorithm for Real-Time Replanning[C]//IJCAI. 1995, 95: 1652-1659.

[4] Adem Tuncer and Mehmet Yildirim, Dynamic path planning of mobile robots with improved genetic algorithm, emphComputers and Electrical Engineering, 38: 1564–1572, 2012.

[5] Hong Qu, Ke Xing and Takacs Alexander, An improved genetic algorithm with co-evolutionary strategy for global path planning of multiple mobile robots, *Neurocomputing*, 120: 509–517, 2013.

[6] Lavalle S M. Rapidly-Exploring Random Trees: A New Tool for Path Planning[J]. Algorithmic & Computational Robotics New Directions, 1999:293–308.

[7] Kuwata Y, Karaman S, Teo J, et al. Real-Time Motion Planning With Applications to Autonomous Urban Driving[J]. IEEE Transactions on Control Systems Technology, 2009, 17(5):1105-1118.

[8] Wangbao Xua, Xuebo Chen, Jie Zhao and Xiaoping Liu, Function-segment artificial moment method for sensor-based path planning of single robot in complex environments, *Information Sciences*, 280: 64–81, 2014.

[9] Ali Noormohammadi Asl, Mohammad Bagher Menhaj and Atena Sajedin, Control of leader–follower formation and path planning of mobile robots using Asexual Reproduction Optimization (ARO), *Applied Soft Computing*, 14, part C: 563–576, 2014.

[10] Morteza Hassanzadeh, Mathias Lidberg, Mansour Keshavarz and Lars Bjelkeflo, Path and Speed Control of a Heavy Vehicle for Collision Avoidance Manoeuvres, *Intelligent Vehicles Symposium, IEEE*, 2012: 129–134.

[11] Liu Wanli, Wang Zhankui and Zhu Hua, Novel Method of Trajectory Tracking and Posture Stabilization for Mobile Robot, in *Proceedings of the 2nd Inernational Asia Conference Information in Control, Automation and Robotics*, 2010: 1–4.

[12] Julio E. Normey-Rico, Ismael Alcal, Juan Gmez-Ortega and Eduardo F. Camacho, Mobile robot path tracking using a robust PID controller, *Control Engineering Practice*, 9(11): 1209–1214, 2001.

[13] Maalouf E, Saad M, Saliah H. A higher level path tracking controller for a four-wheel differentially steered mobile robot[J]. Robotics and Autonomous Systems, 2006, 54(1): 23-33.

[14] Onieva E, Naranjo J E, Milans V, et al. Automatic lateral control for unmanned vehicles via genetic algorithms[J]. Applied Soft Computing, 2011, 11(1):1303-1309.

[15] Attia R, Orjuela R, Basset M. Coupled longitudinal and lateral control strategy improving lateral stability for autonomous vehicle[C]// Proceedings of the American Control Conference. 2012:6509-6514.

[16] Chang S, Gordon T J. Model-based predictive control of vehicle dynamics[J]. International Journal of Vehicle Autonomous Systems, 2007, 5(1).

[17] Di Cairano S, Tseng E, Bernardini D, et al. Steering vehicle control by switched model predictive control[C]//Advances in Automotive Control. 2010: 1-6.

[18] Beal C E, Gerdes J C. Model Predictive Control for Vehicle Stabilization at the Limits of Handling[J]. IEEE Transactions on Control Systems Technology, 2013, 21(21):1258-1269.

[19] Yakub F, Mori Y. Comparative study of autonomous path-following vehicle control via model predictive control and linear quadratic control[J]. Proceedings of the Institution of Mechanical Engineers Part D Journal of Automobile Engineering, 2015, 229(12).